THE JOURNAL OF PHYSICAL CHEMISTRY A LETTERS

2007, *111,* 4122−4124
Published on Web 04/24/2007

Temperature Changes Visualization during Chemical Wave Propagation

Vladimir V. Zhivonitko, Igor V. Koptyug,* and Renad Z. Sagdeev

International Tomography Center, 3A Institutskaya Street, Novosibirsk, 630090, Russia

Received: February 20, 2007; In Final Form: April 10, 2007

Magnetic resonance imaging was used for two-dimensional temperature visualization of chemical waves propagation in the autocatalytic exothermal reaction of thiosulfate oxidation by chlorite. The technique presented is based on the temperature dependence of the water chemical shift. Temperature maps were acquired by employing the TurboFLASH imaging method. The results obtained allow one to judge about directions of buoyancy flows. Two types of convection critical modes in a vertical tube during the wave propagation were detected.

Introduction

Since Luther's discovery[1] of chemical waves in autocatalytic reactions, experimental detection of wave propagation has been based on the variation of physical properties of reactants, products, or intermediates of a chemical reaction and often required the addition of various indicators. Meanwhile, in several autocatalytic reaction systems, considerable temperature changes take place.[2] One such system is based on the oxidation of thiosulfate by chlorite ions (chlorite−thiosulfate system), proceeding in accord with the following equation:

$$S_2O_3^{2-} + 2ClO_2^{-} + H_2O = 2SO_4^{2-} + 2Cl^{-} + 2H^{+} \qquad (1)$$

The reaction is catalyzed by the product hydrogen ion and manifests propagating acidity fronts. Its distinctive feature is a very strong exothermicity, so the temperature change can come to 10 °C, even if concentrations of reagents do not exceed 0.1 M.[2] Such temperature change a priori is large enough to be detected by various techniques, but to the best of our knowledge temperature variation was never used for visualizing the propagation of chemical waves.

Magnetic resonance imaging (MRI) is often used to visualize chemical waves propagation,[3] but MRI thermometry was never employed for this purpose. At the same time, MRI temperature mapping is broadly applied in medicine for noninvasive measurements during ultrasound and thermal surgery.[4] There are two main possibilities often utilized to visualize the temperature of aqueous solutions by nuclear magnetic resonance (NMR). The first one is based on the dependence of relaxation times on temperature.[5] This technique is well established, possibly because of the simple methodology and performance but suffers from poor sensitivity to small temperature changes and the absence of universality in comparison to another one, which is based on the fact that the water proton chemical shift value also depends on temperature.[6] The chemical shift varies linearly with temperature.[7] Generally, a chemical shift change is evaluated by measuring the phase of an NMR signal as a more sensitive parameter that is accessible in MRI. The latter technique was employed in the present work.

In this Letter, the first application of NMR thermometry to measure temperature changes during the chemical wave propagation is presented. Two-dimensional temperature maps were produced for the moving heat front formed in the colorless chlorite−thiosulfate system. Because the relaxation times do not change considerably during this reaction, NMR thermometry appears to be the only MRI technique capable of producing contrast images in this case.

Experimental Section

Chlorite−Thiosulfate System. The highest grades of commercially available $NaClO_2$ (Fluka, 80%), $Na_2S_2O_3$ (Fluka, 99%), and NaOH (Fluka, >98%) were used in the experiments. Because recrystallization of sodium chlorite ($NaClO_2$) to better than 99% purity was reported to have no effect on the kinetics of the chlorite−thiosulfate reaction,[8] all chemicals were used as received. The concentration of sodium chlorite in solution was established iodometrically. The reacting solutions containing 0.025 M $Na_2S_2O_3$, 0.055 M $NaClO_2$, and 0.010 M NaOH were prepared in distilled water. Experiments were performed in a vertically positioned cylindrical glass tube of internal diameter 9.1 mm. The chemical wave was initiated by adding a drop of 0.1 M H_2SO_4 at the top of the tube.

Thermocouple Experiment. A calibrated chromel−copel thermocouple was placed in the center inside the tube with reacting solution. The experiment was performed at ambient temperature (20 °C) outside the superconducting magnet of the NMR instrument. The data were acquired by means of a digital analyzer.

Water Proton Chemical Shift Method. Water proton resonance frequency depends on temperature as a consequence of changes in electronic surroundings of water molecules caused by stretching or bending of hydrogen bonds.[6] Consequently, the chemical shift varies linearly with temperature, with the sensitivity coefficient (α) of about −0.01 ppm/°C over a broad temperature range.[7] Usually, the spatial distribution of water chemical shifts for temperature measurements is not measured

* Corresponding author. E-mail: koptyug@tomo.nsc.ru.

10.1021/jp071435c CCC: $37.00 © 2007 American Chemical Society

directly as a map of resonance frequencies. Instead, the phase of the NMR signal is mapped because its variation can be quantified much more accurately. For the gradient echo sequence often used in such measurements, the temperature dependence of the signal phase is given by the following equation:

$$\Delta\Phi = \gamma \cdot \mathrm{TE} \cdot B_o \cdot \alpha \cdot \Delta T \qquad (2)$$

where γ is the magnetogyric ratio, TE is the echo time, B_o is the macroscopic magnetic induction, and α is the proportionality coefficient that describes the temperature dependence of the water chemical shift. Therefore, temperature variations (ΔT) can be calculated by subtracting the phase distribution ($\Phi(T_o)$) at a reference temperature from the phase distribution after a change in temperature ($\Phi(T)$).[9] To produce temperature maps, as a first approximation it is not necessary to make a new calibration when switching from one solution to another, because the sensitivity coefficient α depends only weakly on the properties of a medium.[9]

Imaging Experiments. MRI experiments were performed on a Bruker DRX-300 spectrometer equipped with a 7.05 T superconducting magnet, operating at a proton resonance frequency of 300 MHz. The tube was imaged using a 25 mm radio frequency coil, which had a maximum vertical observational region of 40 mm. All MRI experiments were carried out at the temperature inside the magnet bore of 18 °C.

Imaging experiments were carried out according to the following methodology. The glass tube with the reaction solution was kept overnight in the superconducting magnet bore of the NMR instrument to get it equilibrated with the bore temperature. After that, the sample was briefly taken out of the magnet, the wave was initiated; then the sample was repositioned in the NMR probe and the experiment was started.

The phase maps were acquired by means of the echo-shifted TurboFLASH (fast low-angle shot) imaging technique.[10,11] An opportunity to make the echo time (TE) longer than the repetition time (TR) is a distinctive feature of this pulse sequence. Therefore acquisition occurs much faster in this case in comparison to conventional gradient echo pulse sequence.[10] The images correspond to slices 2 mm thick positioned at the center of the tube. The following echo-shifted TurboFLASH pulse sequence parameters were used: TE = 19.3 ms, TR = 18.6 ms, flip angle 1.4°, field of view 14 × 39 mm^2 (vertical) and 14 × 16 mm^2 (horizontal). Approximately, 3 s were required for scanning one 64 × 128 (vertical) or 64 × 64 (horizontal) image. Calculation of temperature maps was performed as described above (eq 1).

Results and Discussion

To measure the extent of temperature changes independently, a preliminary thermocouple experiment was performed. The acquired data presented in Figure 1 demonstrate temperature variations which take place during chemical wave propagation in the chlorite−thiosulfate system at the level of reagent concentrations stated above.

The temperature maps corresponding to the vertical and horizontal cross-sections through the center of the tube detected during the evolution of chlorite−thiosulfate system are shown in Figure 2a,b, respectively. According to the data obtained, the value of the temperature change inside the sample correlates quantitatively with the thermocouple measurements shown in Figure 1, if we take into account that in the latter case the thermocouple was located in the center of the tube. Nevertheless, there is one arguable point here. The chemical reaction

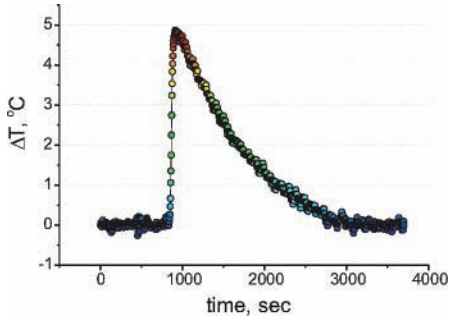

Figure 1. Thermocouple measurements during wave front propagation in the chlorite−thiosulfate system (see text).

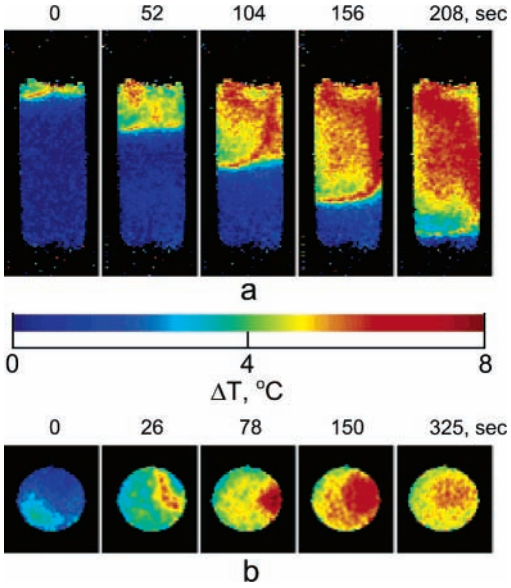

Figure 2. Temperature maps of the propagating chemical wave in the chlorite−thiosulfate system for the vertical (a) and the horizontal (b) cross-sections. The area of images displayed is 14 × 39 mm^2 (a) and 14 × 16 mm^2 (b).

proceeding inside the sample alters the electronic surroundings of water protons. As a consequence, it could lead to a change in chemical shift that is not due to a temperature change. Then MR images would resemble distributions presented in Figure 2a,b. However, it was found that when the reacted solution returns to equilibrium, the water chemical shift returns to its initial value within the experimental error. Therefore, the alteration of solution composition has a negligibly small influence on the measured quantity. The minimum experimental temperature change that could be measured using the applied MRI methodology is estimated from the average phase drift to be ±1 °C.

The acquired data give us an opportunity to judge about directions of buoyancy flows, arising as a result of local heating at the reaction front region. By repeating the same experiment several times, we found that two different types of flow geometries take place in the tube during propagation of the chemical wave in the chlorite−thiosulfate system.

One is the case when warm masses ascend near the wall of the tube (Figure 3a), and another is when warm masses ascend in the central part of the tube (Figure 3b). It is interesting that in some experiments we have observed transformation of these buoyancy flow geometries from one to another, but in most cases the first type (Figure 3a) was found. Existence of similar convection was shown theoretically and in experiments before, in particular by using chemical waves of the Belousov−Zhabotinsky reaction as a passive indicator.[12] According to the

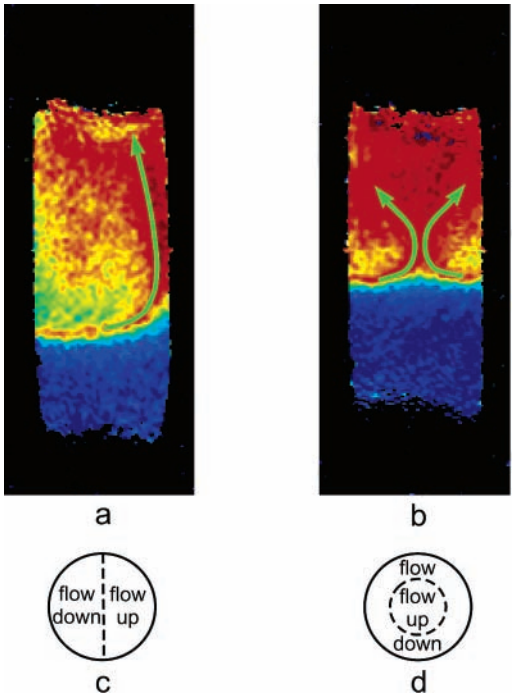

Figure 3. (a), (b) Possible directions of buoyancy flows occurring during the wave propagation in the chlorite-thiosulfate system. (c), (d) Theoretical schematic representation of the first two critical modes of convection for a vertical tube.

paper by Su et al.,[12] the cases presented in Figure 3a,b can be described by the first two critical modes of convection for a vertical tube, shown schematically in Figure 3c,d, respectively. In many cases, convection has considerable influence on stability of chemical waves.[13,14] The MRI technique presented provides a unique possibility to explore these subtle effects directly.

Conclusions

The *reaction−diffusion* model of chemical waves is considered a basic one in the description of many biological,[15] medical,[16] and geophysical[17] events. This work presents the conceptually new detection method of propagating chemical waves based on quantification of temperature changes by means of NMR-thermometry imaging technique. Principally, the technique is based on the measurements of water chemical shift changes caused by temperature variations. A prerequisite for applying this technique is a pronounced exothermicity of a reaction. Temperature changes in excess of 1 °C could be detected in this work with the present implementation of the technique, implying that a reliable visualization of wavefront propagation can be achieved if temperature changes amount to 2−3 °C. Furthermore, it has been demonstrated in the literature[18] that by refining the experimental procedures, the accuracy of temperature evaluations with this technique can be improved to ca. 0.2−0.3 °C.

The work can be extended to the studies of temperature changes in the course of exothermal reactions in aqueous solutions, in general, and thermokinetic autocatalysis,[19] in particular. In addition to temperature mapping, the technique is able to visualize the directions of buoyancy flows. Furthermore, by combining temperature mapping with quantitative MRI velocimetry,[10] it should be possible to obtain information about mass and heat transport during the course of a chemical process in situ practically at the same time.

Acknowledgment. We are grateful for support of the present work by the Russian Foundation for Basic Research (grant 05-03-32472), scientific schools support program (grant NSh-4821.2006.3), Russian Academy of Sciences (grants 5.1.1. and 5.2.3), Siberian Branch of RAS (integration grant #11). I.V.K. thanks the Russian Science Support Foundation for financial support.

References and Notes

(1) Luther, R. Z. *Z. Electrochem.* **1906**, *12*, 596.
(2) Nagypal, I.; Bazsa, G.; Epstein, I. R. *J. Am. Chem. Soc.* **1986**, *108*, 3635−3640.
(3) (a) Tzalmona, A.; Armstrong, R. L.; Menzinger, M.; Cross, A.; Lemaire, C. *Chem. Phys. Lett.* **1992**, *188*, 457−461. (b) Cross, A. R.; Armstrong, R. L.; Reid, A.; Su, S.; Menzinger, M. *J. Phys. Chem.* **1995**, *99*, 16616−16621. (c) Gao, Y.; Cross, A. R.; Armstrong, R. L. *J. Phys. Chem.* **1996**, *100*, 10159−10164. (d) Cross, A. L.; Armstrong, R. L.; Gobrecht, C.; Paton, M.; Ware, C. *Magn. Reson. Imaging* **1997**, *15*, 719−725. (e) Evans, R.; Timmel, C. R.; Hore, P. J.; Britton, M. M. *Chem. Phys. Lett.* **2004**, *397*, 67−72. (f) Britton, M. M.; Sederman, A. J.; Taylor, A. F.; Scott, S. K.; Gladden, L. F. *J. Phys. Chem. A* **2005**, *109*, 8306−8313. (g) Evans, R.; Timmel, C. R.; Hore, P. J.; Britton, M. M. *J. Amer. Chem. Soc.* **2006**, *128*, 7309−7314. (h) Britton, M. M. *J. Phys. Chem.* **2006**, *110*, 2579−2582.
(4) (a) Kuroda, K.; Chung, A. H.; Hynynen, K.; Jolesz, F. A. *J. Magn. Reson. Imaging* **1998**, *8*, 175−181. (b) Cline, H. E.; Schenck, J. F.; Watkins, R. D.; Hynynen, K.; Jolesz, F. A. *Magn. Reson. Med.* **1993**, *30*, 98−106.
(5) *Encyclopedia of nuclear magnetic resonance*; Grant, D. M.; Harris, R. K. Eds.; Wiley: New York, 1996; Vol. 7, pp 4689−4692.
(6) (a) Schneider, W. G.; Bernstein, H. J.; Pople, J. A. *J. Chem. Phys.* **1958**, *28*, 601−607. (b) Muller, N. *J. Chem. Phys.* **1965**, *43*, 2555−2556.
(7) Hindman, J. C. *J. Chem. Phys* **1966**, *44*, 4582−4592.
(8) Nagypal, I.; Epstein, I. R.; Kustin, K. *Int. J. Chem. Kinet.* **1986**, *18*, 345−353.
(9) (a) Ishihara, Y.; Calderon, A.; Watanabe, H.; Okamoto, K.; Suzuki, Y.; Kuroda, K.; Suzuki, Y. *Magn. Reson. Med.* **1995**, *34*, 814−823. (b) Nott, K. P.; Hall, L. D.; Bows, J. R.; Hale, M.; Patrick, M. L. *Magn. Res. Imaging* **2000**, *18*, 69−79.
(10) Callaghan, P. T. *Principles of Nuclear Magnetic Resonance Microscopy*; Clarendon Press: Oxford, U.K., 1991.
(11) Harth, Th.; Kahn, T.; Rassek, M.; Schwabe, B.; Schwarzmaier, H.; Lewin, J. S.; Muodder, U. *Magn. Reson. Med.* **1997**, *38*, 238−245.
(12) Su, S.; Armstrong, R. L.; Menzinger, M.; Cross, A.; Lemaire, C. *J. Chem. Phys.* **1993**, *98*, 7295−7300.
(13) (a) Menzinger, M.; Tzalmona, A.; Armstrong, R. L.; Cross, A.; Lemaire, C. *J. Phys. Chem.* **1992**, *96*, 4725−4727. (b) Britton, M. M. *J. Phys. Chem. A* **2003**, *107*, 5033−5041. (c) Pojman, J. A.; Nagy, I. P.; Epstein, I. R. *J. Phys. Chem.* **1991**, *95*, 1306−1311.
(14) Pojman, J. A.; Epstein, I. R. *J. Phys. Chem.* **1990**, *94*, 4966−4972.
(15) (a) Lee, K. J.; Goldstein, R. E.; Cox, E. C. *Phys. Rev. Lett.* **2001**, *6*, 068101 (4 pages). (b) Bugrim, A. E.; Zhabotinsky, A. M.; Epstein, I. R. *Biophys. J.* **1997**, *73*, 2897−2906.
(16) Biktasheva, I. V.; Biktashev, V. N.; Dawes, W. N.; Holden, A. V.; Saumarez, R. C.; Savill, A. M. *Int. J. Bifurcation Chaos* **2003**, *13*, 3645−3655.
(17) (a) Malchow, H. *J. Marine Syst.* **1996**, *7*, 193−202. (b) Tang, Sh.; Wu, J.; Cui, M. *Commun. Nonlin. Sci. Num. Simul.* **1996**, *1*, 27−31.
(18) (a) De Poorter, J.; De Wagter, C.; De Deene, Y.; Thomsen, C.; Stahlberg, F.; Achten, E. *J. Magn. Reson. B* **1994**, *103*, 234−241. (b) Wlodarczyk, W.; Boroschewski, R.; Henyschel, M.; Wust, P.; Monich, G.; Felix, R. *J. Magn. Reson. Imaging* **1998**, *8*, 165−174.
(19) Pojman, J. A.; Craven, R.; Khan, A.; West, W. *J. Phys. Chem.* **1992**, *96*, 7466−7472.